Continuous Fluorescence Assay of Phytochrome Assembly *in Vitro*†

Liming Li,‡,§ John T. Murphy,§ and J. Clark Lagarias*

Section of Molecular and Cellular Biology, University of California, Davis, California 95616

Received February 28, 1995; Revised Manuscript Received April 17, 1995⊗

ABSTRACT: Incubation of recombinant apophytochrome with the phycobiliprotein chromophore precursor phycoerythrobilin produces a covalent adduct that exhibits a fluorescence excitation maximum at 576 nm and an emission maximum at 586 nm. Using these fluorescence parameters, we have developed a kinetic assay for quantitative analysis of the assembly of the plant photoreceptor phytochrome in real time. Kinetic measurements performed with different phycoerythrobilin concentrations confirm that bilin attachment to apophytochrome involves two steps, an initial formation of a reversible non-covalent complex followed by thioether bond formation. The kinetic constants for both steps of phycoerythrobilin attachment to apophytochrome were estimated with this assay. Methodology for determining the kinetic constants for the assembly of both the natural phytochrome chromophore precursor, phytochromobilin, and the analog phycocyanobilin is also described. Since the latter two bilins yield covalent, nonfluorescent adducts with apophytochrome, their co-incubation with phycoerythrobilin reduces the rate of formation of the fluorescent phycoerythrobilin adduct in an irreversible, competitive manner. Competition experiments were also performed with biliverdin, a structurally related bilin which does not form a covalent adduct with apophytochrome. Such measurements show that biliverdin reversibly binds to apophytochrome with a submicromolar binding constant, an affinity which is very similar to that of phytochromobilin. The utility of this fluorescence assay for identification of novel inhibitors of phytochrome assembly and for characterization of the structural features of both bilin and apophytochrome necessary for photoreceptor assembly is discussed.

The ability to adjust to changes in the external light conditions is especially important to photosynthetic organisms. Plants therefore possess numerous photoreceptors which perceive the direction, wavelength, and intensity of light in their natural environment. Action spectroscopy has defined three major families of plant photoreceptors—those which regulate responses to UV-B, blue/UV-A, and red regions of the electromagnetic spectrum (Kendrick & Kronenberg, 1994). Phytochrome, a mediator of photomorphogenic responses primarily to red and far-red light, is the best characterized of these photoreceptor families. The phytochrome molecule consists of a polypeptide of roughly 1100 amino acids to which the linear tetrapyrrole prosthetic group phytochromobilin (PΦB)[1] is thioether-linked (Quail, 1991; Terry et al., 1993b). The bilin chromophore confers upon phytochrome the unique ability to photointerconvert between two stable isomers, a red light absorbing form, Pr, and a far-red light absorbing form, Pfr (Rudiger & Thummler, 1991). The photointerconversion between these two forms initiates or reverses the biochemical cascade which culminates in the particular photoadaptive response at the organismal level.

Since phytochrome regulates many important photomorphogenic responses, such as seed germination, flower induction, and senescence, the biochemical processes involved in its biosynthesis are obvious targets for regulation of plant growth and development (Terry et al., 1993b). For this reason, the final step of phytochrome biosynthesis, the ligation of PΦB to the phytochrome apoprotein, is of considerable interest for targeting regulators of plant photomorphogenesis. The ability to reconstitute photochemically active holophytochrome *in vitro* using recombinant apophytochrome and various bilin pigments has facilitated biochemical dissection of this assembly process (Deforce et al., 1991, 1993; Hill et al., 1994; Kunkel et al., 1993; Lagarias & Lagarias, 1989; Wahleithner et al., 1991). Many of these studies have exploited a sensitive zinc-dependent fluorescence assay for detection of the covalent linkage between the two components (Berkelman & Lagarias, 1986). Such methodology has helped define structural features of both bilin (Li & Lagarias, 1992) and apophytochrome (Deforce et al., 1993) that are necessary for the assembly of holophytochrome.

In the present investigation, we describe a novel kinetic assay for quantitative analysis of the assembly of the plant photoreceptor phytochrome *in vitro*. This assay exploits the visible fluorescence of the bilin−apophytochrome adduct which is produced when recombinant apophytochrome is incubated with the chromophore analog phycoerythrobilin (PEB). Unlike the zinc-dependent fluorescence assay for phytochrome assembly, bilin attachment can be monitored in real time, which greatly simplifies the experimental

† This work was supported by a grant (AMD-9203377) from the United States Department of Agriculture Competitive Research Grants Program and by an NIH training grant (to J.T.M., Grant 5 T32 GM07377-17).

* To whom correspondence should be addressed: Section of Molecular and Cellular Biology, University of California, Davis, CA 95616. Tel: (916)-752-1865. FAX: (916)-752-3085. E-mail: jclagarias@ucdavis.edu.

‡ Current address: Department of Molecular and Cellular Biology, Harvard University, Cambridge, MA 02138.

§ These two authors contributed equally to this work.

⊗ Abstract published in *Advance ACS Abstracts,* June 1, 1995.

[1] Abbreviations: BV, biliverdin IXα; Pr, the red light absorbing form of phytochrome; Pfr, the far-red light absorbing form of phytochrome; PCB, phycocyanobilin; PEB, phycoerythrobilin; PΦB, phytochromobilin; TFA, trifluoroacetic acid.

0006-2960/95/0434-7923$09.00/0

measurement of the assembly kinetics. The new assay has facilitated measurement of the dissociation constants and catalytic rate constants for apophytochrome assembly with natural as well as nonnatural chromophore precursors. These investigations provide new insight into the mechanism of bilin assembly, extending conclusions made earlier (Li & Lagarias, 1992).

EXPERIMENTAL PROCEDURES

Bilin Preparations. Crude phycocyanobilin (PCB) was prepared from lyophilized *Spirulina platensis* as described previously (Terry et al., 1993a). Crude PΦB and PEB were prepared by methanolysis of acetone-treated *Porphyridium cruentum* cells (Cornejo et al., 1992). Purification of 3E-PCB, 3E-PEB and 3E-PΦB was accomplished by reverse-phase HPLC (Li & Lagarias, 1992). Biliverdin IXα (BV) was prepared from bilirubin as described previously (Elich et al., 1989). Stock solutions of all purified bilins were prepared in Me_2SO to afford a final concentration of approximately 1−1.5 mM. Concentrations of bilin stock solutions were determined spectrophotometrically after dilution of an aliquot into 2% HCl (v/v) in MeOH. The following molar absorption coefficients in HCl−MeOH were used to estimate bilin concentrations: 30.8 mM^{-1} cm^{-1} at 696 nm for BV (McDonagh, 1979), 38 mM^{-1} cm^{-1} at 680 nm for 3E-PCB (Cole et al., 1967), 25.2 mM^{-1} cm^{-1} at 594 nm for 3E-PEB (Chapman et al., 1967), and 38 mM^{-1} cm^{-1} at 708 nm for 3E-PΦB (Weller & Gossauer, 1980).

Apophytochrome Preparations. The yeast expression plasmids pMphyA3 and pMphyA11 containing the respective sense and antisense orientations of the oat phytochrome A cDNA were expressed in *Saccharomyces cerevisiae* strain 29A (MATα leu2-3 leu2-112 his3-1 ade1-101 trp1-289) essentially as described (Wahleithner et al., 1991). A few plasmid-bearing yeast colonies were inoculated into 3 mL of synthetic raffinose (SR) selective media [0.67% (w/v) yeast nitrogen base without amino acids, 2% (w/v) raffinose, and 40 mg L^{-1} each of adenine, histidine, and tryptophan] and grown overnight at 30 °C with shaking at 300 rpm. Three of these overnight cultures were used to inoculate 1 L of fresh SR medium. After the cultures had grown to an approximate OD_{580} of 0.5, galactose was added to give a final concentration of 1% (w/v) in order to induce apophytochrome expression. Yeast cells were harvested 24 h after galactose addition, and apophytochrome was partially purified from cell homogenates as described previously (Wahleithner et al., 1991). The concentration of "ligation-competent" apophytochrome in each yeast protein extract was estimated spectrophotometrically after incubation of an aliquot with PCB (Li & Lagarias, 1992). Apophytochrome-containing protein extracts in TEGE buffer [10 mM Tris-HCl, pH 8.0, containing 25% (v/v) ethylene glycol and 1 mM EDTA] containing 1 mM phenylmethanesulfonyl fluoride and 1 mM dithiothreitol were frozen in liquid N_2 and stored at −80 °C.

Standard Fluorescence Assay for PEB−Phytochrome Adduct Formation. The formation of the fluorescent PEB-phytochrome adduct was initiated in a polystyrene microcuvette (Fisher Ultra-Vu) by addition of ≥70-fold molar excess of PEB (typically 0.5−15 μM final concentration) to an apophytochrome solution (10 nM final concentration of ligation-competent apophytochrome) in TEGE buffer containing 1 mM phenylmethanesulfonyl fluoride and 1 mM DTT at room temperature. The PEB was dissolved in Me_2SO, and the final Me_2SO concentration in the assay cuvette was adjusted to 1−2%. After rapid mixing by inverting the cuvette a few times, time-based fluorescence measurements were performed as described under Fluorescence Measurements. Raw fluorescence data was stored as an ASCII text file and analyzed using Microsoft Excel as described in Results. In brief, this analysis involved the following steps. The fraction of apophytochrome remaining at each time point was first calculated by dividing the fluorescence observed at a given time by the fluorescence measured at saturation (*i.e.*, when all of the apophytochrome molecules had assembled with PEB). The latter was determined by incubating a control apophytochrome sample with a very large excess of PEB (*i.e.*, >500-fold molar excess) for >1 h. The same saturating fluorescence value could also be obtained by prolonged incubation of each experimental reaction mixture. A semilog plot of the percent apophytochrome remaining as a function of time was then constructed from this normalized data. The slope of this plot in the 5−100-s region was used to estimate the apparent rate constant (k_{app}) for the formation of the PEB−phytochrome adduct under the particular experimental condition being tested. A double-reciprocal plot of $1/k_{app}$ versus 1/[PEB] was then used to estimate K_{PEB} and k_2 from the x- and y-intercept, respectively.

Competitive Fluorescence Kinetic Assay for Holophytochrome Assembly. The competitive assays were performed essentially as described above with the following modifications. The apophytochrome solutions (10 nM final concentration of ligation-competent apophytochrome) in TEGE buffer containing 1 mM phenylmethanesulfonyl fluoride and 1 mM DTT were first preequilibrated to room temperature in polystyrene microcuvettes. For the BV competition experiments, various amounts of BV (0.5−5 μM final concentration) were added to individual apophytochrome solutions, mixed by gentle inversion, and incubated for 30 s. Time-based fluorescence measurements were initiated following addition of PEB to a final concentration of 3 μM as described under Fluorescence Measurements. Kinetic data was analyzed using Microsoft Excel as described in Results. In brief, this analysis involved the following steps. The kinetic data for each BV concentration was used to estimate k_{app} for the formation of the PEB−phytochrome adduct as described above. The BV dissociation constant (K_i) was calculated from the x-intercept of the plot of $1/k_{app}$ versus BV concentration using the values for K_{PEB} and k_2 determined with the standard fluorescence assay for PEB−phytochrome adduct formation. For PCB and PΦB competition experiments, time-based fluorescence acquisitions were initiated immediately after the addition of a premixed solution containing a fixed amount of PEB (3−4 μM final concentration) and different amounts of competitor bilin (0.067−1.0 μM final concentration of PCB or PΦB). In all cases, the final Me_2SO concentration was kept constant between 1 and 2% (v/v) for all samples within an individual competitor concentration series experiment. Kinetic data was analyzed using Microsoft Excel as described in Results. In brief, this analysis involved the following steps. The kinetic data for each competitor bilin concentration (*i.e.*, PCB or PΦB) was used to determine k_{app} for the formation of the PEB−phytochrome adduct as described above. The rate constant for the formation of the nonfluorescent bilin−apophyto-

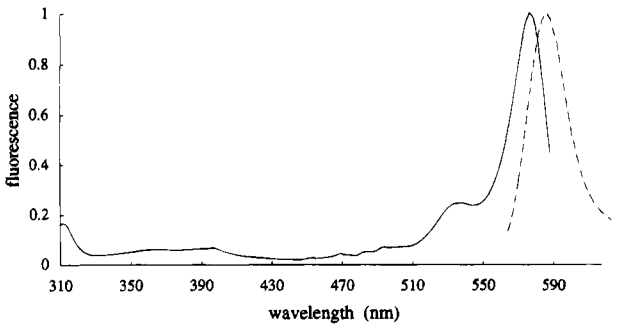

FIGURE 1: Fluorescence excitation and emission spectra of PEB−phytochrome adduct. A yeast extract containing 90 nM apophytochrome was assembled with a 10-fold molar excess of PEB in TEGE buffer as described under Experimental Procedures. Solid line, normalized fluorescence excitation spectrum (emission wavelength 600 nm); dashed line, normalized fluorescence emission spectrum (excitation wavelength 530 nm).

chrome adduct (k_{app}^{i}) was obtained by subtracting the measured K_{bilin} value from that determined in the absence of competitor bilin. A double-reciprocal plot of $1/k_{app}^{i}$ versus 1/[bilin] was then used to estimate the dissociation constant (K_i) and the catalytic rate constant (k_4) from the x- and y-intercept, respectively.

Fluorescence Measurements. All fluorescence measurements were taken at 22−25 °C with an SLM 8000C fluorescence spectrophotometer. Samples were placed in polystyrene microcuvettes (Fisher Ultra-Vu), which were excited through the 1 cm path length direction. For standard excitation and emission spectra, the spectral resolution was adjusted to 2 nm with the excitation and emission band-passes being respectively set to 2 and 16 nm. For time-based measurements, the following fluorescence spectrophotometer settings were used: 2-nm resolution, excitation wavelength at 570 nm, emission wavelength at 586 nm, 1-s integration time, excitation band-pass of 2 nm, and emission band-pass of 16 nm. Data was typically collected for 15−30 min.

Protein Assay. Protein concentrations were determined using the BCA protein assay (Pierce Chemical Co.) with BSA as a standard (Smith et al., 1985).

RESULTS

Fluorescence Properties of the PEB−Phytochrome Adduct. We previously reported that several ethylidene-containing bilins could spontaneously form covalent adducts with recombinant oat apophytochrome A (Li & Lagarias, 1992). One of these pigments was the phycobiliprotein chromophore precursor, phycoerythrobilin (PEB), which differs from PΦB by the reduction of the C15=C16 double bond. That study also demonstrated that the PEB−phytochrome adduct is photochemically inactive. This result is consistent with the hypothesis that photoisomerization of the C15=C16 double bond is the primary mechanism of the Pr to Pfr photointerconversion (Rudiger et al., 1983). The efficiency of this photoisomerization process accounts for the observation that native oat phytochrome has a very weak intrinsic fluorescence (Colombano et al., 1990). Since light absorbed by the PEB−phytochrome adduct cannot be released via C15=C16 double bond isomerization, we predicted that this species would be fluorescent. Figure 1 demonstrates that the PEB−phytochrome adduct is indeed fluorescent, with an excitation maximum at 576 nm and an emission maximum at 586 nm. To verify that these fluorescence spectra represent the PEB−phytochrome adduct, soluble protein extracts from yeast cells containing the antisense phytochrome plasmid were similarly analyzed. These measurements provided no evidence for such a fluorescent species, nor could this species be detected in the apophytochrome A extract or PEB preparations when analyzed separately. Experiments were next performed to determine whether these fluorescence properties could be used for quantitative analysis of the amount of the PEB−phytochrome adduct. For this purpose, a dilution series of PEB−phytochrome adduct was prepared and the concentration dependence of the fluorescence intensity at 586 nm was determined. This experiment demonstrated that fluorescence intensity is a linear function of the amount of PEB−phytochrome adduct within the concentration range of 0.5−20 nM (data not shown).

Scheme 1: Kinetic Analysis of Holophytochrome Assembly

$$\text{bilin} + \text{apoPC} \underset{k_{-1}}{\overset{k_1}{\rightleftharpoons}} \text{bilin:apoPC} \xrightarrow{k_2} \text{bilin–PC}$$

$$\frac{-d[\text{apoPC}]_T}{dt} = k_2[\text{bilin:apoPC}] \quad (1)$$

$$[\text{apoPC}]_T = [\text{apoPC}] + [\text{bilin:apoPC}]$$

$$K_{bilin} = \frac{[\text{bilin}][\text{apoPC}]}{[\text{bilin:apoPC}]}$$

Combining the above equations,

$$\frac{-d[\text{apoPC}]_T}{dt} = k_2\left[\frac{[\text{bilin}]}{K_{bilin} + [\text{bilin}]}\right][\text{apoPC}]_T \quad (2)$$

When [bilin] >> [apoPC],

$$= k_{app}[\text{apoPC}]_T$$

Integrating,

$$\ln\left[\frac{[\text{apoPC}]_t}{[\text{apoPC}]_0}\right] = -k_{app}t \quad (3)$$

where

$$k_{app} = k_2\left[\frac{[\text{bilin}]}{K_{bilin} + [\text{bilin}]}\right] \quad (4)$$

Rearranging,

$$\frac{1}{k_{app}} = \frac{K_{bilin}}{k_2}\frac{1}{[\text{bilin}]} + \frac{1}{k_2} \quad (5)$$

Kinetic Analysis of PEB Attachment to Apophytochrome. We have proposed that holophytochrome assembly consists of two steps as shown in Scheme 1—a binding step, where a non-covalent bilin−apophytochrome complex is produced, followed by a catalytic step, where the thioether linkage is achieved (Li & Lagarias, 1992). Such a mechanism resembles that proposed for the attachment of PCB to apophycocyanin in which a rapid non-covalent bilin−apoprotein association precedes a slower bilin attachment reaction (Arciero et al., 1988a). While data presented in earlier studies are consistent with this mechanism (Deforce et al., 1993; Kunkel et al., 1993; Li & Lagarias, 1992), none of these investigations have addressed this question directly. Experimental confirmation of this mechanism requires performing the assembly reaction at several different bilin concentrations. As outlined in Scheme 1, the kinetics of bilin−apophytochrome adduct formation should obey the rate expression defined by eq 2. Assuming that the bilin

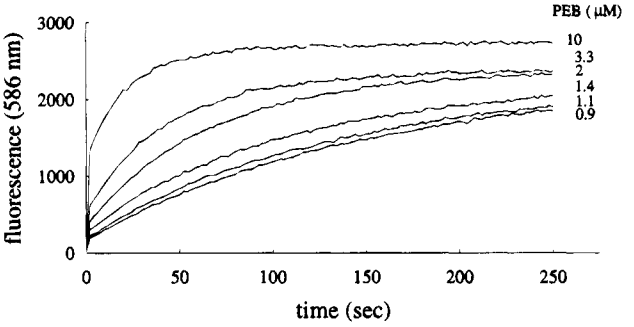

FIGURE 2: Time course of the formation of the PEB−phytochrome adduct. Yeast extracts containing 10 nM apophytochrome were incubated with various concentrations of PEB as described under Experimental Procedures. The PEB concentrations are indicated to the right of the respective curves.

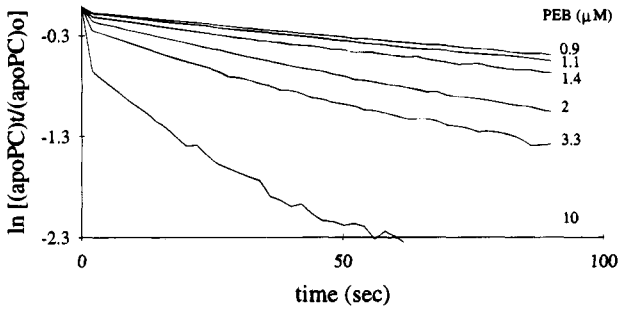

FIGURE 3: Determination of apparent rate constants for PEB−phytochrome assembly. The curves shown in Figure 2 were replotted according to eq 3 (see Scheme 1). The k_{app} values for assembly at each PEB concentration were determined from the slopes of these lines. PEB concentrations are indicated to the right of the respective curves.

precursor concentration is kept constant, semilog plots of the fraction of apophytochrome remaining are expected to be linear as defined by eq 3. Previous studies have already established that phytochrome assembly obeys this pseudo-first-order kinetic description (Deforce et al., 1993; Li & Lagarias, 1992). Scheme 1 also predicts that the observed rate constant for bilin attachment (k_{app}) will be a function of the bilin concentration, its affinity for apophytochrome (K_{bilin}), and the catalytic rate constant k_2 according to eq 4. We have defined K_{bilin} to represent the equilibrium dissociation constant for the non-covalent binding of bilin to apophytochrome; hence this analysis assumes that the initial bilin binding step is at equilibrium. The reciprocal form of eq 4 (*i.e.*, eq 5) provides a very useful means to obtain both kinetic constants from plots of $1/k_{app}$ versus 1/[PEB]. Non-zero x- and y-intercepts of such plots will thus provide direct experimental support for the two-step mechanism proposed in Scheme 1.

Since the fluorescence of the PEB−phytochrome adduct can be used to experimentally monitor the rate of PEB attachment to apophytochrome, we first performed experiments to analyze the assembly of PEB to apophytochrome. Figures 2−4 show the analysis of a representative experiment in which apophytochrome was incubated with a range of 90−1000-fold molar excess of PEB. Figure 2 clearly shows that the level of 586-nm fluorescence increased with time as the PEB−phytochrome adduct was produced. When PEB was omitted from the reaction mixture, no measurable increase of 586-nm fluorescence was observed during the same time period (data not shown). Figure 2 also demonstrates that the rate of PEB-adduct formation was dependent on the PEB

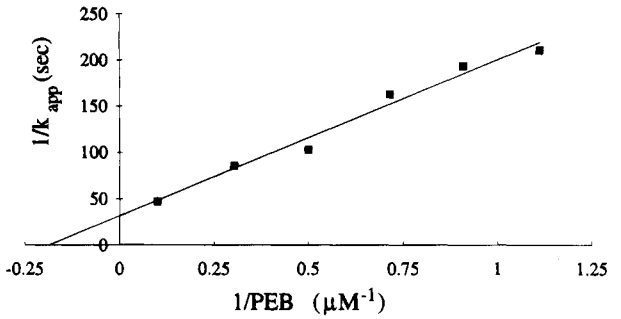

FIGURE 4: Determination of the equilibrium dissociation constant and catalytic rate constant for PEB−phytochrome assembly. PEB concentrations are plotted as a reciprocal against the reciprocal of the k_{app} values (*i.e.*, slopes) derived from Figure 3. The x- and y-intercepts were used according to eq 5 to determine $K_{PEB} = 5.32$ μM and $k_2 = 0.03$ s^{-1} for the experiment shown (see Scheme 1).

Table 1: Kinetic Constants for Phytochrome Assembly[a]

bilin	K_{bilin} (μM)	k_{cat} (s^{-1})	n
PΦB	1.02 ± 0.13	0.30 ± 0.01	2
PCB	1.31 ± 0.05	0.25 ± 0.02	2
PEB	7.93 ± 1.63	0.054 ± 0.015	5
BV	0.89 ± 0.33	N/A	4

[a] The bilin dissociation constants (K_{bilin}) and catalytic rate constants (k_{cat}) for apophytochrome assembly with various substrates are shown. Constants were derived from multiple experiments performed as described in the figures and Experimental Procedures. The mean values (±SD) from each set of experiments are shown. N/A indicates measurements that do not apply, and n refers to the number of experiments considered in each case.

concentration, and that the final fluorescence intensity reached a limiting value. With the highest PEB concentration tested (*i.e.*, 10 μM PEB), this saturating fluorescence intensity occurred within 5 min. The reactions performed with lower PEB concentrations eventually reached the same fluorescence intensity but only after prolonged incubation times (data not shown). This saturating value was therefore used to estimate the amount of ligatable apophytochrome that was present at any time during the reaction. As predicted in Scheme 1, semilog plots of the fraction of apophytochrome remaining proved to be linear throughout 90% of the ligation reaction as shown in Figure 3. The pseudo-first-order rate constants, k_{app}, for each PEB concentration were derived from the slope of each line between 10 and 100 s. These values were used to construct the double-reciprocal plot shown in Figure 4. The two kinetic constants, K_{PEB} and k_2, were then obtained from the respective x- and y-intercepts according to eq 5. For the experiment shown in Figure 2, K_{PEB} and k_2 were estimated to be 5.32 μM and 0.03 s^{-1}, respectively. The results of five independent experiments are summarized in Table 1. From these experiments, the average values for K_{PEB} and k_2 were determined to be 7.93 μM and 0.054 s^{-1}, respectively.

BV as a Competitive Inhibitor of PEB-Phytochrome Assembly. We previously demonstrated that BV does not form a covalent adduct with apophytochrome because it lacks the ethylidene group on the A-ring (Li & Lagarias, 1992). Given the fact that BV and PΦB are structurally similar, it is likely that BV will exhibit a strong affinity for the chromophore binding site on apophytochrome. BV is therefore expected to be a reversible, competitive inhibitor of PEB attachment. Scheme 2 proposes a kinetic model for

Scheme 2: Reversible, Competitive Inhibition of PEB Phytochrome Assembly by BV

$$\text{BV:apoPC} \underset{k_{-3}}{\overset{k_3}{\rightleftharpoons}} \text{BV} + \text{apoPC} + \text{PEB} \underset{k_{-1}}{\overset{k_1}{\rightleftharpoons}}$$

$$\text{PEB:apoPC} \xrightarrow{k_2} \text{PEB–PC}$$

$$\frac{-\text{d[apoPC]}_T}{dt} = k_2[\text{PEB:apoPC}] \quad (6)$$

where

$$[\text{apoPC}]_T = [\text{apoPC}] + [\text{PEB:apoPC}] + [\text{BV:apoPC}]$$

$$K_{PEB} = \frac{[\text{PEB}][\text{apoPC}]}{[\text{PEB:apoPC}]} \qquad K_{BV} = \frac{[\text{BV}][\text{apoPC}]}{[\text{BV:apoPC}]}$$

Combining the above equations,

$$\frac{-\text{d[apoPC]}_T}{dt} = \left[\frac{k_2[\text{PEB}]K_{BV}}{K_{PEB}K_{BV} + K_{BV}[\text{PEB}] + K_{PEB}[\text{BV}]}\right][\text{apoPC}]_T \quad (7)$$

When [PEB] and [BV] >> [apoPC],

$$= k_{app}[\text{apoPC}]_T$$

Integrating,

$$\ln\left[\frac{[\text{apoPC}]_t}{[\text{apoPC}]_0}\right] = -k_{app}t \quad (8)$$

where

$$k_{app} = \left[\frac{k_2[\text{PEB}]K_{BV}}{K_{PEB}K_{BV} + K_{BV}[\text{PEB}] + K_{PEB}[\text{BV}]}\right] \quad (9)$$

Rearranging,

$$\frac{1}{k_{app}} = \left[\frac{K_{PEB}}{K_{BV}k_2[\text{PEB}]}\right][\text{BV}] + \left[\frac{K_{PEB} + [\text{PEB}]}{k_2[\text{PEB}]}\right] \quad (10)$$

PEB adduct formation in the presence of BV. Figures 5–7 show a representative BV competition assembly experiment analyzed according to this kinetic model. In this experiment, constant concentrations of apophytochrome (10 nM) and PEB (3 μM) were incubated with six different BV concentrations over the range 0.5–5 μM. These concentrations were chosen to ensure that both bilin concentrations remain effectively constant throughout the kinetic analysis. The raw fluorescence data is shown in Figure 5. These results clearly demonstrate that the rate of formation of the PEB–phytochrome adduct is inhibited with increasing BV concentration. Semilog replots of each data set shown in Figure 6 reveal that PEB assembly obeys pseudo-first-order kinetics under all experimental conditions tested as predicted by eq 7 (Scheme 2). From the slopes of each line, k_{app} values for the PEB–phytochrome assembly were determined. These values were used to construct the plot shown in Figure 7 according to eq 10 (Scheme 2). The x-intercept of this plot yielded an estimate of the equilibrium dissociation constant for BV (K_{BV}) to be 0.90 μM for this experiment. On the basis of four independent experiments, the average value for K_{BV} was estimated to be 0.89 μM. Scheme 2 also predicts that the amount of PEB–phytochrome adduct produced at infinite time should reach the same saturating value for all BV concentrations tested. Our experiments revealed that the amount of PEB–phytochrome fluorescence approached the same final value regardless of the BV concentration tested (Figure 5 and data not shown). Taken together, these results

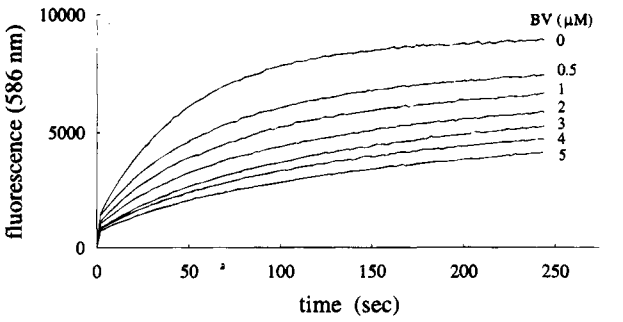

FIGURE 5: Time course of the reversible, competitive inhibition of PEB–phytochrome assembly by BV. Yeast extracts containing 10 nM apophytochrome were preincubated for 30 s with various concentrations of BV as indicated to the right of each curve. Time-based fluorescence measurements were initiated upon addition of PEB (final concentration 3 μM) as described under Experimental Procedures.

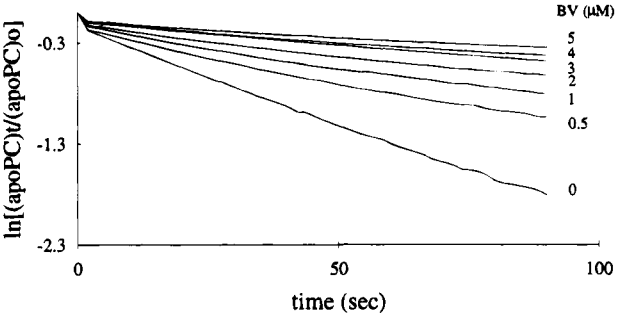

FIGURE 6: Determination of apparent rate constants for PEB–phytochrome assembly in the presence of BV competitor. The slopes of these lines were used to calculate k_{app} values as described in Figure 3.

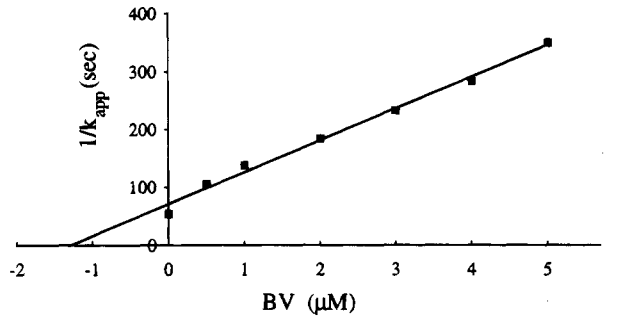

FIGURE 7: Determination of the equilibrium dissociation constant for BV. BV concentrations were plotted against the reciprocal of the k_{app} values (*i.e.*, slopes) derived from Figure 6 according to eq 10 (see Scheme 2). The *x*-intercept value was used to estimate k_{BV} to be 0.9 μM for this experiment.

support the model in which BV is a reversible, competitive inhibitor for phytochrome assembly.

PΦB and PCB as Irreversible Inhibitors of PEB–Phytochrome Assembly. On the basis of the above BV experiments, we reasoned that PΦB and its analog PCB would also inhibit the formation of the PEB–phytochrome adduct via their ability to form covalent adducts with apophytochrome (Li & Lagarias, 1992). The kinetic model for this type of irreversible competition is proposed in Scheme 3. With this analysis, the binding constants and catalytic rate constants for attachment of each bilin to apophytochrome can be determined. These experiments require that the PΦB and PCB adducts do not themselves fluoresce at the wavelength used to detect the formation of

Scheme 3: Irreversible Inhibition of PEB Phytochrome Assembly by PΦB and PCB

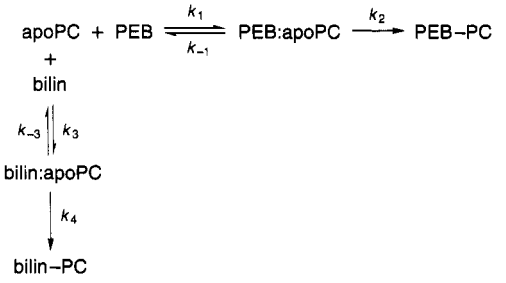

$$K_{PEB} = \frac{[PEB][apoPC]}{[PEB:apoPC]} \qquad K_i = \frac{[bilin][apoPC]}{[bilin:apoPC]}$$

When [PEB] >> [apoPC] and [bilin] >> [apoPC],

$$\frac{d[PEB-PC]}{dt} = k_2\left[\frac{[PEB]}{K_{PEB} + [PEB]}\right][apoPC]_T = k_{app}[apoPC]_T \quad (11)$$

$$\frac{d[bilin-PC]}{dt} = k_4\left[\frac{[bilin]}{K_i + [bilin]}\right][apoPC]_T = k_{app}^I[apoPC]_T \quad (12)$$

Therefore,

$$\frac{[PEB-PC]}{[bilin-PC]} = \frac{k_{app}}{k_{app}^I} \quad (13)$$

where

$$k_{app}^I = k_4\left[\frac{[bilin]}{K_i + [bilin]}\right] \quad (14)$$

Rearranging,

$$\frac{1}{k_{app}^I} = \frac{1}{[bilin]}\frac{K_i}{k_4} + \frac{1}{k_4} \quad (15)$$

the PEB−phytochrome adduct. To test this assumption, PΦB and PCB were incubated with apophytochrome A under conditions where the respective covalent adducts were produced. During this incubation period, no significant fluorescence emission at 586 nm was detected, thus confirming that the PΦB and PCB adducts are not fluorescent under these assay conditions (data not shown).

According to the kinetic model shown in Scheme 3, the formation of both PEB−phytochrome adduct and competitor bilin−phytochrome adducts is defined by the respective rate expressions, eqs 11 and 12. These equations mathemetically represent first-order rate expressions as long as the concentrations of all bilin species are held constant. This was achieved by using a large (*i.e.*, >70-fold) molar excess of each bilin to apophytochrome in the assay mixture. When both PΦB and PEB are present in the reaction mixture, the two bilins compete irreversibly for binding to apophytochrome. Although the amount of PEB adduct produced can be determined by fluorescence, the concentration of bilin−phytochrome adduct cannot. The latter can easily be determined, however, since the ratio of the rates of formation of both adducts is equal to the ratio of the corresponding pseudo-first-order rate constants as defined by eq 13 (Scheme 3). Experimentally, the amount of competitor bilin adduct can be estimated from the degree of fluorescence inhibition relative to a control reaction where the irreversible inhibitor (*i.e.*, PΦB or PCB) was omitted from the reaction mixture. The k_{app}^i values can be calculated using eq 13 and then plotted as a function of competitor bilin concentration according to eqs 14 and 15 (Scheme 3). If the irreversible

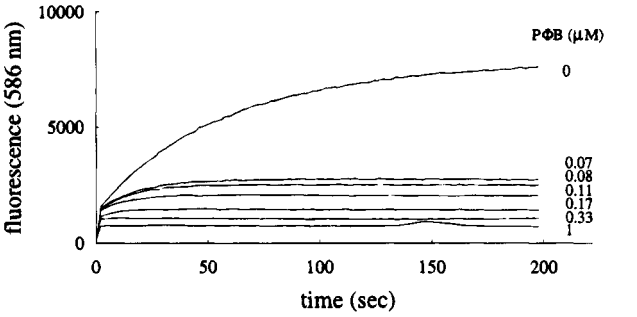

FIGURE 8: Time course of the irreversible inhibition of PEB−phytochrome assembly by PΦB. Yeast extracts containing 10 nM apophytochrome were incubated with a premixed solution of PΦB and PEB as described under Experimental Procedures. The final concentration of PEB was 3.0 μM, and various concentrations of PΦB are indicated to the right of the acquired curves.

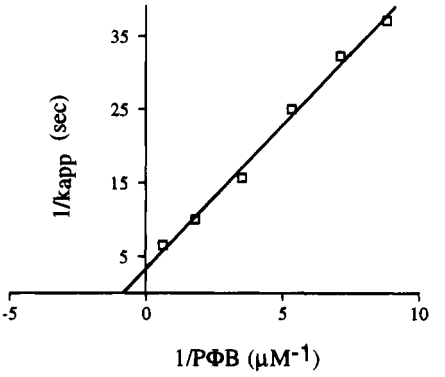

FIGURE 9: Determination of the equilibrium dissociation constant and catalytic rate constant for inhibition of PEB−phytochrome assembly by PΦB. Double reciprocal replots of $1/k_{app}^i$ versus 1/[PΦB] were determined as described under Experimental Procedures and Results. The *x*- and *y*-intercepts were used according to eq 15 to determine $K_i^{P\Phi B} = 1.14$ μM and $k_4^{P\Phi B} = 0.31$ s^{-1} for the experiment shown (see Scheme 3).

competitive kinetic model is correct, then plots of $1/k_{app}^i$ versus 1/[bilin] should afford estimates of both equilibrium dissociation constants (K_{bilin}) as well as catalytic rate constants (k_4) for the ligation of both PΦB and PCB to apophytochrome.

In Figures 8 and 9, data from a representative experiment using PΦB as the inhibitor of PEB assembly is presented. The raw fluorescence data is presented in Figure 8. These experiments indicate that the rate of formation of the PEB adduct was significantly inhibited by increasing amounts of PΦB. In addition, the reduced level of PEB adduct fluorescence at saturation clearly demonstrates that PΦB binding had irreversibly precluded the attachment of PEB. The apparent rate constants, k_{app}, for PΦB assembly at each corresponding concentration of PΦB were calculated according to eq 13, and the measured value for k_{app} determined in the absence of PΦB. This information was then used to construct the double-reciprocal plot shown in Figure 9. On the basis of this plot and eq 15 (Scheme 3), the PΦB dissociation constant ($K_i^{P\Phi B}$) and the catalytic rate constant ($k_4^{P\Phi B}$) for attachment of PΦB to apophytochrome were determined to be 1.14 μM and 0.31 s^{-1}, respectively. On the basis of two independent experiments, average values for $K_i^{P\Phi B}$ and $k_4^{P\Phi B}$ were estimated to be 1.02 μM and 0.30 s^{-1}, respectively. A similar kinetic analysis was performed with the chromophore analog PCB (data not shown). On the basis of two independent experiments, average values

of K_i^{PCB} and k_4^{PCB} were determined to be 1.31 μM and 0.25 s^{-1}, respectively. These results support the mechanistic model presented in Scheme 3 in which PΦB and PCB assemble with apophytochrome in a two-step reaction.

DISCUSSION

In this study, we have established that the covalent adduct produced between oat apophytochrome A and PEB is fluorescent, with an excitation maximum at 576 nm and an emission maximum at 586 nm. This result is consistent with our prediction that removal of the photochemically active C15=C16 double bond will significantly increase the quantum yield of phytochrome fluorescence. The fluorescence properties of the PEB−phytochrome adduct are similar to those of C-phycoerythrins, a family of light-harvesting phycobiliproteins from cyanobacteria which contain five covalently linked PEB prosthetic groups (Glazer, 1989). The fluorescence emission spectra of both proteins display similar peak structures (*i.e.*, narrow band width with a long-wavelength shoulder) and similarly sized Stokes' shifts (*i.e.*, 10 nm). These features of the two fluorescence spectra indicate that the PEB chromophores are rigidly bound to both biliproteins. Interestingly, the emission maximum of the PEB−phytochrome adduct is red-shifted by nearly 10 nm relative to that of the longest wavelength emitting C-phycoerythrin known (Glazer, 1989). This observation is consistent with the hypothesis that the chromophore of the PEB−phytochrome adduct has a more extended configuration. Previously, we and others have argued that the P_r phytochrome chromophore adopts an *E,anti* configuration at the C10 methine bridge (Fodor et al., 1990), which is more extended than the C_{10}-*Z,syn* geometry of the PEB prosthetic groups of C-phycoerythrin and phycoerythrocyanin (Duerring et al., 1991; Ficner & Huber, 1993; Ficner et al., 1992). The longer wavelength emission maximum of the PEB−phytochrome adduct could also be rationalized by differences in the local protein environment in the two biliproteins (*i.e.*, effects of nearby charged and/or nonpolar residues). The above analysis is based on the assumption that the chemical structure or linkage of the PEB prosthetic group of the phytochrome adduct is the same as those found in the phycobiliproteins. Since nonenzymatic attachment of PEB to recombinant apophycocyanin and apophycoerythrin mainly yields oxidized bilin adducts with red-shifted emission spectra (Arciero et al., 1988b; Fairchild & Glazer, 1994), we cannot dismiss this possibility *a priori*. A detailed chemical analysis of the chromophore of the PEB−phytochrome adduct will be required to resolve this issue.

On the basis of the fluorescence properties of the PEB−phytochrome adduct, we have developed novel assay methodologies for kinetic analysis of phytochrome assembly. Our fluorescence assay is extremely sensitive, yielding an easily detectable signal for adduct concentrations as low as 0.5 nM. In addition, the formation of the covalent linkage can be continuously monitored in real time, which is a vast improvement from the zinc-dependent fluorescence blot analysis described previously (Li & Lagarias, 1992). This has enabled us to experimentally verify that bilin attachment to apophytochrome occurs in two steps, a reversible non-covalent association followed by covalent bond formation as proposed in Scheme 1. In this study, we have compared the kinetics of the attachment of the natural PΦB prosthetic group and two chromophore analogs, PCB and PEB. The values for the bilin dissociation constants and catalytic rate constants obtained here are in good agreement with the apparent rate constants determined earlier using the zinc blot analysis (Li & Lagarias, 1992). Of the three bilins, PΦB exhibits the greatest affinity for apophytochrome with a dissociation constant of 1.02 μM, compared with 1.31 and 7.93 μM for K_{PCB} and K_{PEB}, respectively. These values indicate that PCB and PΦB bind to apophytochrome with similar affinities, while PEB has a considerably reduced binding affinity. The rotational freedom of the C15 methine bridge of PEB likely accounts for this phenomenon by lowering the concentration of the ligation-competent conformer(s). Comparison of the catalytic rate constants for covalent attachment of the three bilins to apophytochrome provides additional supporting evidence that PΦB is the preferred bilin substrate on catalytic grounds. In this regard, PΦB exhibits the largest value for k_{cat} of 0.30 s^{-1}, compared with 0.25 and 0.054 s^{-1} for PCB and PEB, respectively. The reduced rate constants for the two PΦB analogs are probably due to the conformational distortion of catalytic residues in apophytochrome which are required to accommodate the binding of these unnatural bilins. For PEB, this could also reflect the reduced electrophilicity of the A ring ethylidene caused by the loss of the C15=C16 double bond. Taken together, these studies corroborate and extend the conclusion made earlier that the chromophore binding site on apophytochrome A is optimally tailored to the natural chromophore precursor PΦB (Li & Lagarias, 1992).

The kinetic constants for phytochrome assembly reported in this study provide additional insight into the mechanism of this reaction. The experimental observation that k_{app} is a hyperbolic function of the bilin concentration (*i.e.*, eqs 4 and 14 in Schemes 1 and 3, respectively) supports the interpretation that the catalytic step is rate limiting at all bilin concentrations tested. On the basis of the value determined for the catalytic rate constant for PΦB of 0.3 s^{-1} and the lowest concentration of PΦB used in this study (*i.e.*, 67 nM), we estimate that the bimolecular rate constant for PΦB binding to apophytochrome (*i.e.*, k_1 or k_3 in Schemes 1 and 3, respectively) must be at least 4.5×10^6 M^{-1} s^{-1}. This suggests that the non-covalent association of PΦB with apophytochrome occurs very rapidly, with a rate constant approaching the diffusion limit of 10^9 M^{-1} s^{-1}. These limiting values for k_1 confine the rate constant for PΦB dissociation from the non-covalent PΦB:apophytochrome intermediate (*i.e.*, k_{-1} or k_{-3} in Schemes 1 and 3) to lie between 4.5 and 1000 s^{-1} given the PΦB dissociation constant of 1.02 μM determined in this study. On the basis of these considerations, the rapid equilibrium assumption for the initial PΦB binding step appears to be satisfied. Verification of this conclusion will however require the experimental determination of k_1 and k_{-1}, which is beyond the scope of the present investigation. An additional insight provided by our kinetic measurements relates to the potential interaction between the two bilin binding subunits of the apophytochrome dimer. It is well established that phytochrome is a homodimer, and recombinant apophytochrome appears to be a dimer as well (Edgerton & Jones, 1993; Ito et al., 1991). It is thus conceivable that bilin attachment to one subunit will affect the rate of attachment to the other. We see no evidence for such intersubunit cooperativity during bilin attachment. This result is consistent with the structural model for phytochrome in which the two chro-

mophore binding domains are non-interacting (Tokutomi et al., 1989).

The micromolar dissociation constant for PΦB indicates that apophytochrome has a very high affinity for the natural chromophore *in vivo*. Since the apophytochrome preparations used in this study contain other yeast proteins, however, the effective free bilin concentrations may actually be smaller than that specified due to bilin association with these non-phytochrome polypeptides. Thus, the true binding affinity of PΦB may even be greater than that determined in this investigation. Resolution of this question awaits the purification of recombinant apophytochrome to homogeneity. Plant cells may also contain factors which regulate the rate of phytochrome assembly by their ability to alter the affinity or catalytic rate constant for the attachment of PΦB to apophytochrome. The fluorescence assay presented in this study should prove useful for the identification and characterization of such novel regulatory molecules. One such regulatory molecule may be BV, which has a binding affinity very similar to that of PΦB itself (see Table 1). Since BV is the biosynthetic precursor of PΦB in plant cells (Terry et al., 1993b), this observation suggests that BV could act as a natural inhibitor of phytochrome assembly *in vivo*. The biological importance of this type of inhibition to the regulation of phytochrome levels depends upon the relative concentrations of BV and PΦB at the site of phytochrome assembly as well as the relative rates of apophytochrome synthesis and turnover. Holophytochrome assembly is thought to occur in the cytoplasm, where the mature photoreceptor is predominantly localized. Bilin trafficking from the site of synthesis in the plastid to the cytoplasm therefore may play a significant role in the regulation of phytochrome assembly.

The fluorescence assay methodology described in this study will facilitate further dissection of the mechanism of phytochrome assembly. The pH and temperature dependence of phytochrome assembly kinetics should provide new insight into the nature of ionizable groups as well as the thermodynamics of both the binding and the catalysis steps. We also expect that this methodology will prove especially useful for determining the role that individual residues play in the binding or the catalysis steps using site-directed mutagenesis of apophytochrome. A site-directed mutagenesis study was recently described which utilized the zinc blot assay to determine apparent rate constants of assembly (Deforce et al., 1993). The continuous fluorescence assay developed here should enhance mutant analysis by differentiating the involvement of particular amino acids with repect to bilin binding or catalysis. In addition, assembly studies with various phytochrome family members may reveal kinetic differences which could have important implications with regard to regulation of light-mediated plant growth and development.

ACKNOWLEDGMENTS

We thank Dr. Dave Deamer for the use of his spectrofluorimeter facility and Dr. Irwin H. Segel for helpful discussions.

REFERENCES

Arciero, D. M., Bryant, D. A., & Glazer, A. N. (1988a) *J. Biol. Chem. 263*, 18343−18349.

Arciero, D. M., Dallas, J. L., & Glazer, A. N. (1988b) *J. Biol. Chem. 263*, 18350−18357.

Berkelman, T. R., & Lagarias, J. C. (1986) *Anal. Biochem. 156*, 194−201.

Chapman, D. J., Cole, W. J., & Siegelman, H. W. (1967) *J. Am. Chem. Soc. 89*, 5976−5977.

Cole, W. J., Chapman, D. J., & Siegelman, H. W. (1967) *J. Am. Chem. Soc. 89*, 3643−3645.

Colombano, C. G., Braslavsky, S. E., Holzwarth, A. R., & Schaffner, K. (1990) *Photochem. Photobiol. 52*, 19−22.

Cornejo, J., Beale, S. I., Terry, M. J., & Lagarias, J. C. (1992) *J. Biol. Chem. 267*, 14790−14798.

Deforce, L., Tomizawa, K. I., Ito, N., Farrens, D., Song, P. S., & Furuya, M. (1991) *Proc. Natl. Acad. Sci. U.S.A. 88*, 10392−10396.

Deforce, L., Furuya, M., & Song, P. S. (1993) *Biochemistry 32*, 14165−14172.

Duerring, M., Schmidt, G. B., & Huber, R. (1991) *J. Mol. Biol. 217*, 577−592.

Edgerton, M. D., & Jones, A. M. (1993) *Biochemistry 32*, 8239−8245.

Elich, T. D., McDonagh, A. F., Palma, L. A., & Lagarias, J. C. (1989) *J. Biol. Chem. 264*, 183−189.

Fairchild, C. D., & Glazer, A. N. (1994) *J. Biol. Chem. 269*, 28988−28996.

Ficner, R., & Huber, R. (1993) *Eur. J. Biochem. 218*, 103−106.

Ficner, R., Lobeck, K., Schmidt, G., & Huber, R. (1992) *J. Mol. Biol. 228*, 935−950.

Fodor, S. P. A., Lagarias, J. C., & Mathies, R. A. (1990) *Biochemistry 29*, 11141−11146.

Glazer, A. N. (1989) *J. Biol. Chem. 264*, 1−4.

Hill, C., Gartner, W., Towner, P., Braslavsky, S. E., & Schaffner, K. (1994) *Eur. J. Biochem. 223*, 69−77.

Ito, N., Tomizawa, K., & Furuya, M. (1991) *Plant Cell Physiol. 32*, 891−895.

Kendrick, R. E., & Kronenberg, G. H. M. (1994) *Photomorphogenesis in Plants*, 2nd ed., Martinus Nijhoff Publishers, Dordrecht, The Netherlands.

Kunkel, T., Tomizawa, K., Kern, R., Furuya, M., Chua, N. H., & Schafer, E. (1993) *Eur. J. Biochem. 215*, 587−594.

Lagarias, J. C., & Lagarias, D. M. (1989) *Proc. Natl. Acad. Sci. U.S.A. 86*, 5778−5780.

Li, L. M., & Lagarias, J. C. (1992) *J. Biol. Chem. 267*, 19204−19210.

McDonagh, A. F. (1979) in *The Porphyrins* (Dolphin, D., Ed.) pp 293−491, Academic Press, New York.

Quail, P. H. (1991) *Annu. Rev. Genet. 25*, 389−409.

Rudiger, W., & Thummler, F. (1991) *Angew. Chem., Intl. Ed. Engl. 30*, 1216−1228.

Rudiger, W., Thummler, F., Cmiel, E., & Schneider, S. (1983) *Proc. Natl. Acad. Sci. U.S.A. 80*, 6244−6248.

Smith, P. K., Krohn, R. I., Hemanson, G. T., Mallia, A. K., Gartner, F. H., Provenzano, M. D., Fujimoto, E. K., Goeke, N. M., Olsen, B. J., & Klenk, D. C. (1985) *Anal. Biochem. 150*, 76−85.

Terry, M. J., Maines, M. D., & Lagarias, J. C. (1993a) *J. Biol. Chem. 268*, 26099−26106.

Terry, M. J., Wahleithner, J. A., & Lagarias, J. C. (1993b) *Arch. Biochem. Biophys. 306*, 1−15.

Tokutomi, S., Nakasako, M., Sakai, J., Kataoka, M., Yamamoto, K., Wada, M., Tokunaga, F., & Furuya, M. (1989) *FEBS Lett. 247*, 139−142.

Wahleithner, J. A., Li, L., & Lagarias, J. C. (1991) *Proc. Natl. Acad. Sci. U.S.A. 88*, 10387−10391.

Weller, J. P., & Gossauer, A. (1980) *Chem. Ber. 113*, 1603−1611.

BI950453U